Monthly Notices of the ROYAL ASTRONOMICAL SOCIETY
MNRAS Advance Access published March 23, 2013
MNRAS (2013)
Advance Access publication
doi:10.1093/mnras/stt361

Spectral properties of two-component advective flows with standing shocks in the presence of Comptonization

Santanu Mondal[1]⋆ and Sandip K. Chakrabarti[1,2]

[1]*Indian Centre for Space Physics, Chalantika 43, Garia Station Road, Kolkata 700084, India*
[2]*S. N. Bose National Centre for Basic Sciences, Salt Lake, Kolkata 700098, India*

Accepted 2013 February 25. Received 2013 January 27; in original form 2012 November 10

ABSTRACT

We study self-consistently the hydrodynamic and spectral properties of a general class of steady-state accretion discs where we couple both the hydrodynamics and the radiative transfer. We consider a two-component accretion flow in which the Keplerian disc is immersed inside an accreting low angular momentum flow (halo) around a black hole. The injected soft photons from the Keplerian disc are reprocessed by the electrons in the halo. We study the transonic properties of such a Comptonized flow. We use the Rankine–Hugoniot relation to obtain the shock locations in the disc and compute the radiated spectrum from this shocked disc. We identify the boundary of the parameter space spanned by the specific energy and angular momentum which allows the formation of the standing shocks. We show how the boundary changes in the presence of Compton cooling. Due to the radiative loss, some energy is removed from the accreting matter and the shock moves towards the black hole to maintain the pressure balance condition. We solve the two-temperature equations with Coulomb energy exchange between the protons and the electrons, and the radiative processes such as the bremsstrahlung and thermal Comptonization. We study the variation of the hydrodynamical and spectral properties as a function of the accretion rates of the Keplerian and sub-Keplerian components. Ours is the most accurate transonic solution of an inviscid flow around a black hole to date.

Key words: accretion, accretion discs – black hole physics – hydrodynamics – shock waves.

1 INTRODUCTION

A black hole accretion is necessarily transonic (e.g. Liang & Thompson 1980; Paczyński & Witta 1980; Paczyński & Bisnovatyi-Kogan 1981; Chakrabarti 1990c, hereafter C90c). However, till date, no transonic flow solution has been obtained in the presence of thermal Comptonization. It is well established that in the context of stellar mass black holes, the hard X-rays are produced by the Comptonization of soft X-rays (Sunyaev & Titarchuk 1980, 1985; hereafter ST80 and ST85, respectively). Observers realized that a complete picture must have the standard Keplerian disc (Novikov & Thorne 1973; Shakura & Sunyaev 1973) which produces the soft photons, and a hot corona (ST80; ST85; Haardt & Maraschi 1993; Zdziarski et al. 2003), or the unstable inner edge of the standard disc (Kobayashi et al. 2003) which Comptonized the soft photons. The latter component is called the Compton cloud. Theoretical solutions of transonic flows indicate that the so-called Compton cloud cannot be anything other than the post-shock region of the low angular momentum flow which can accompany the Keplerian component (Chakrabarti & Titarchuk 1995, hereafter CT95), making the flow essentially of two components, one Keplerian and the other sub-Keplerian. The post-shock region of the latter component is known as the CENBOL, or CENtrifugal pressure supported BOundary Layer, since for all practical purposes, this layer dissipates heat through thermal Comptonization and produces observable hard radiation. Furthermore, the CENBOL could be responsible for the outflows or jets, like any other boundary layers (Chakrabarti 1998, 1999).

In CT95, spectral properties of the two-component advective flow (TCAF) around black holes were studied. However, the shock location was chosen as a parameter and was not computed from ab initio calculation. Every spectrum was computed for a set of accretion rates of the Keplerian component ($\dot{m}_{\rm d}$), the sub-Keplerian component ($\dot{m}_{\rm h}$) and the shock location. The Comptonization was included in the post-shock (CENBOL) region. It was shown that with the increase in $\dot{m}_{\rm d}$, which increases the soft photon flux from the Keplerian disc, the spectrum softens. In contrast, with an increase in $\dot{m}_{\rm h}$, which increases the number of electrons in the CENBOL, the spectrum hardens.

The hydrodynamic properties of a TCAF solution is actually governed by two basic solutions of the transonic flow: one is the inviscid solution (Chakrabarti 1989, hereafter C89) which showed that a significant region of the parameter space allows the

⋆ E-mail: santanuicsp@gmail.com

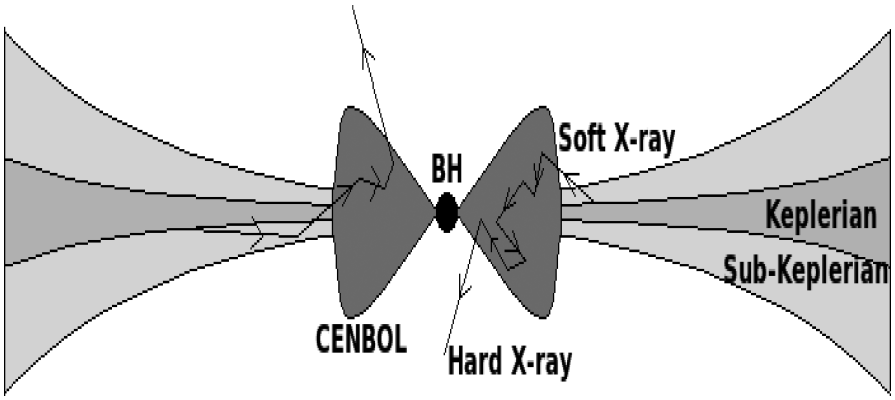

Figure 1. A cartoon diagram of the geometry of an accretion flow. The zigzag trajectories are the typical paths followed by the soft photons from the Keplerian disc. These photons are Comptonized by the CENBOL (post-shock region of the sub-Keplerian flow) and are radiated as hard X-rays.

formation of standing shocks in the accretion flow. The inner part of the flow, till the inner sonic point which is located around three Schwarzschild radii, is supersonic and almost freely falling. In C90b and Chakrabarti (1996a,b), the flow properties in the presence of viscosity were studied and it was found that the flow above a critical value of the Shakura–Sunyaev viscosity parameter α_c can become Keplerian and enter into the black hole after passing through the inner sonic point. This flow cannot have any shock. However, a flow with $\alpha < \alpha_c$ can produce a standing shock in the disc. Thus, a generalized flow having a higher viscosity parameter on the equatorial plane would automatically produce the two-component flow where the Keplerian disc is segregated in the region of higher α surrounded by the remaining lower α flow. In both these basic solutions, however, the cooling due to Comptonization was not included. The inclusion of bremsstrahlung cooling (Molteni, Sponholz & Chakrabarti 1996; Das & Chakrabarti 2004) showed that the shock advanced closer to the black hole due to the loss of thermal pressure. Recently, Giri & Chakrabarti (2013) have demonstrated using numerical simulations that a TCAF solution is indeed formed and is stable.

In the present paper, we resolve several outstanding issues. The questions we attempt to answer are: (a) How does the sonic points of the flow and the shock locations change in the presence of thermal Comptonization? (b) How would the resulting spectrum depend on the accretion rates of the Keplerian and sub-Keplerian components? In the next section, we present the resulting equations and discuss the procedure to solve these equations. In Section 3, we present the results. Finally, in Section 4, we draw the concluding remarks. We do not include the so-called bulk motion Comptonization in deriving the spectrum as the effects will remain practically unchanged over and above what is described in CT95, Titarchuk & Zannias (1998) and Laurent & Titarchuk (1999). Consequently, the spectral saturation of black hole candidates as claimed by Shaposhnikov & Titarchuk (2009), Titarchuk & Seifina (2009) and Laurent & Titarchuk (2011) will remain unchanged.

2 GEOMETRY OF THE MODEL AND BASIC EQUATIONS

Our basic goal is to present a complete transonic flow solution in the presence of Comptonization in black hole geometry. Consider a thin, low angular momentum, axisymmetric flow around the black hole on its equatorial plane. The geometry around the black hole is described by the Paczyński & Witta (1980) pseudo-Newtonian potential $\Phi_{\rm PN} = -\frac{1}{2(r-1)}$. We use the geometric unit $G = M = c = 1$. The radial distances and specific angular momenta are measured in units of $r_{\rm s} = 2GM/c^2$ and $cr_{\rm s} = 2GM/c$, respectively. To supply with the soft (seed) photons for Comptonization, we assume a Keplerian disc on the equatorial plane, truncated at the shock radius. This disc emits a flux of radiation same as that produced by a Shakura & Sunyaev (1973) disc. In Fig. 1, we present a cartoon diagram of the two-component model where a Keplerian disc resides at the equatorial plane and it is surrounded by the sub-Keplerian flow which we call a halo. At the centre of the coordinate, a black hole of mass $M_{\rm BH}$ is located. In the case of a thin flow, there can be two sonic points (C89) which may allow the formation of a shock transition (a discontinuous jump from the supersonic to the subsonic branch). The soft photons emerging from the Keplerian disc are reprocessed via Compton or inverse Compton scattering within the post-shock region. An injected photon may undergo a single, multiple or no scattering at all with hot electrons in between its emergence from the Keplerian disc and its escape from the halo. The photons that enter the black holes are absorbed.

2.1 Flux of soft photons

The soft photons are produced from a Keplerian disc. The soft photons obey a multicolour blackbody spectrum coming from a standard (Shakura & Sunyaev 1973, hereafter SS73) disc. We assume the disc to be optically thick and the opacity due to free–free absorption is more important than the opacity due to scattering. The emission is blackbody type with the local surface temperature (SS73). In our case, the Keplerian disc emits a flux $F_{\rm ss}$ of Shapiro & Teukolosky (1984) from the shock till the outer edge:

$$F_{\rm ss} = 7.6 \times 10^{26} r^{-3} \Im \left(\frac{M_{\rm bh}}{\rm M_\odot}\right) \frac{\dot{M}}{1.4 \times 10^{17}} {\rm erg\,cm^{-2}\,s^{-1}}. \quad (1)$$

Here, $\Im = 1 - (3/r)^{1/2}$. In the above equation, the mass of the black hole $M_{\rm bh}$ is measured in units of the mass of the Sun ($\rm M_\odot$) and the disc accretion rate $\dot{M}$ is in units of gm $\rm s^{-1}$. We assume $M_{\rm bh} = 5$ in the rest of the paper.

2.2 Hydrodynamic equations governing the transonic flows

We consider axisymmetric matter accreting on the equatorial plane of a Schwarzschild black hole. The radial momentum equation is

given by (C89):

$$v\frac{\mathrm{d}v}{\mathrm{d}r}+\frac{1}{\rho}\frac{\mathrm{d}P}{\mathrm{d}r}-\frac{\lambda^2}{r^3}+\phi'(r)=0. \tag{2}$$

Integrating this, we get the specific energy of the flow,

$$\varepsilon=\frac{v^2}{2}+na^2+\frac{\lambda^2}{2r^2}-\frac{(r-1)^{-1}}{2}, \tag{3}$$

where P and ρ are the thermal pressure and density, respectively, λ is the specific angular momentum, v is the infall velocity, $n=\frac{1}{(\gamma-1)}$ is the polytropic index, $a=\sqrt{(\frac{\gamma P}{\rho})}$ and $\phi(r)=-\frac{(r-1)^{-1}}{2}$ denotes the Paczyński & Witta (1980) potential which mimics the geometry of the black hole quite well. The mass conservation equation, up to a constant, is given by

$$\dot{M}=\rho vrh(r). \tag{4}$$

It is useful to rewrite this equation in terms of v and a in the following way:

$$\dot{\mathcal{M}}=va^q f(r), \tag{5}$$

where $q=(\gamma+1)/(\gamma-1)$ and $f(r)=r^{3/2}(r-1)$ for the vertical flow. Here, $\dot{\mathcal{M}}$ is the entropy accretion rate (C89) which is conserved for an ideal flow but can vary at the shock front.

2.2.1 *Shock condition and shock constant*

Angular momentum of the halo causes a centrifugal barrier to form. Matter piles up behind this barrier and forms a shock (C89; Chakrabarti 1990b, hereafter C90b; C90c). The post-shock region, which acts as a boundary layer, becomes hot as the kinetic energy of the pre-shock flow is converted into the thermal energy. This region is called the CENBOL. Being hot, the CENBOL is puffed up and intercepts soft photons from the Keplerian disc (CT95). If the intercepted soft-photon number is high enough, the CENBOL is cooled down due to inverse Comptonization. The optically-thin pre-shock halo does not radiate efficiently; therefore, energy and entropy are advected with the flow. Due to the loss of energy at the shock front, the shock condition for the black hole accretion flow is

$$\varepsilon_+=\varepsilon_--\Delta\varepsilon, \tag{6a}$$

where $\Delta\varepsilon$ is the energy loss due to Comptonization. This is basically a function of the electrons and low-energy photons and can be calculated for different accretion rates of the flow. The baryon number conservation of the flow gives

$$\dot{M}_+=\dot{M}_-. \tag{6b}$$

The pressure balance condition, which suggests that the sum of the thermal pressure and ram pressure match on both sides of the shock (C89), is given by

$$W_++\Sigma_+v_+^2=W_-+\Sigma_-v_-^2, \tag{6c}$$

where W and Σ are the pressure and density, integrated in the vertical direction (Matsumoto et al. 1984). The subscripts '−' and '+' denote the pre-shock and post-shock quantities, respectively. To get the locations of the shock, it is better to express the flow parameters in terms of some invariant quantities. For this, rewrite the equations (6a), (5) and (6c) in terms of the Mach number $M=\frac{v}{a}$ of the flow,

$$\frac{1}{2}M_+^2a_+^2+\frac{a_+^2}{\gamma-1}=\frac{1}{2}M_-^2a_-^2+\frac{a_-^2}{\gamma-1}-\Delta\varepsilon, \tag{7a}$$

$$\dot{\mathcal{M}}_+=M_+a_+^{\nu}f(r_\mathrm{s}), \tag{7b}$$

$$\dot{\mathcal{M}}_-=M_-a_-^{\nu}f(r_\mathrm{s}) \tag{7c}$$

and

$$\frac{a_+^{\nu}}{\dot{\mathcal{M}}_+}\left[\frac{2\gamma}{3\gamma-1}+\gamma M_+^2\right]=\frac{a_-^{\nu}}{\dot{\mathcal{M}}_-}\left[\frac{2\gamma}{3\gamma-1}+\gamma M_-^2\right], \tag{7d}$$

where $\nu=\frac{3\gamma-1}{\gamma-1}$ and r_s is the location of the shock. After some algebra, from the above Rankine–Hugoniot condition, we obtain the Mach number relation which connects the pre-shock and post-shock (C90b) quantities:

$$\frac{[M_+(3\gamma-1)+(2/M_+)]^2}{2+(\gamma-1)M_+^2}=\frac{[M_-(3\gamma-1)+(2/M_-)]^2}{2+(\gamma-1)M_-^2-\frac{2\Delta\varepsilon(\gamma-1)}{a_-^2}}. \tag{8a}$$

M_-^2 can be evaluated using equations (7a)–(7c):

$$M_-^2=\frac{(\frac{\dot{\mathcal{M}}_+M_-}{\dot{\mathcal{M}}_-M_+})^{1/4}[2+(\gamma-1)M_+^2]-2}{(\gamma-1)}+\frac{2\Delta\varepsilon}{a_-^2}. \tag{8b}$$

However, if the flow were one-dimensional (cylindrical with constant height or of conical shape having a constant wedge angle), then a different Mach number relation would be followed (Chakrabarti 1990a, hereafter C90a; Das, Chakrabarti & Mondal 2010; Singh & Chakrabarti 2011):

$$\frac{[M_+\gamma+(1/M_+)]^2}{2+(\gamma-1)M_+^2}=\frac{[M_-\gamma+(1/M_-)]^2}{2+(\gamma-1)M_-^2-\frac{2\Delta\varepsilon(\gamma-1)}{a_-^2}}. \tag{9}$$

When the energy loss takes place instantaneously at the shock location, the shock condition becomes different (Singh & Chakrabarti 2011). However, in our case, the energy is lost all over the CENBOL region, and thus the modification of the shock condition from that of a non-dissipative flow is not required. Hence, we continue to use equation (8) as the invariant Mach number relation.

2.3 Radiative processes and governing equations

As the matter accretes, it is compressed due to geometrical effects and becomes hotter. At the same time, electrons lose energy due to bremsstrahlung and Comptonization of the soft photons from the disc. They also gain energy from protons due to Coulomb interaction and as a result the protons are cooled down. The energy equation that the protons and electrons obey in the post-shock region is

$$\frac{\partial(\varepsilon+\frac{P}{\rho})}{\partial r}+(\Gamma-\Lambda)=0, \tag{10}$$

where ε is given by equation (3), and Γ and Λ are the heating and cooling terms, respectively. If the electron temperature T_e is high enough, $kT_\mathrm{e}>m_\mathrm{e}c^2$, we use $\gamma=4/3$; otherwise, we use $\gamma=5/3$. We ignore the synchrotron cooling because this requires the knowledge of the unknown magnetic field configuration. In this paper, we also ignore the pair production and annihilation effects. The bremsstrahlung and the Coulomb terms are taken from the standard text (e.g. Lang 1980). The Comptonization rate is taken from CT95. In this paper, we mainly concentrate on the thermal Comptonization process as prescribed in CT95, and for the sake of completeness, the details of the processes are given below. During Comptonization, the energy exchange takes place through the scattering of photons off the free electrons. As the scattering is increased and the Thomson opacity

$$\tau_\mathrm{T}=\int_{r_i}^{\infty}\sigma_\mathrm{T}n_\mathrm{e}\,\mathrm{d}r \tag{11}$$

approaches unity, the escaping photon acquires energy due to repeated scattering with the hot electrons. The average energy exchange per scattering is given by ($h\nu$, $kT_{\rm e} \ll m_{\rm e}c^2$)

$$\frac{\Delta\nu}{\nu} = \frac{4kT_{\rm e} - h\nu}{m_{\rm e}c^2}. \tag{12}$$

When $h\nu \ll kT_{\rm e}$, photons gain energy due to the Doppler effect. As the radiation passes through the medium, the probability of repeated scattering by the same photon decreases exponentially although the corresponding gain in energy is exponentially higher. A balance between these two factors yields a power-law distribution of the energy density:

$$F_\nu \propto \nu^{-\alpha}. \tag{13}$$

Titarchuk & Lyubarskij (1995) gave a prescription to calculate the spectral index (α) for a wide range of optical depths and electron temperatures of a plasma cloud. This is given by the recursion relation

$$\alpha = \frac{\beta}{\ln\left[1 + (\alpha+3)\Theta/(1+\Theta) + 4d_0^{1/\alpha}\Theta^2\right]}, \tag{14}$$

where

$$d_0(\alpha) = \frac{3[(\alpha+3)\alpha+4]\Gamma(2\alpha+2)}{(\alpha+2)(\alpha+3)^2} \tag{15}$$

and $\Theta = kT_{\rm e}/m_{\rm e}c^2$ which represents the average dimensionless temperature of the electron in the post-shock region normalized with respect to the rest-mass energy of the electron. The factor β can be calculated using $\xi = \exp(-\beta)$ which is the eigenvalue in the corresponding radiative transfer problem (ST80; ST85). The form of the parameter β, if we consider the post-shock region as a slab (Titarchuk 1994; CT95), for an optical depth $\tau_0 > 0.1$ is

$$\beta = \frac{\pi^2(1-{\rm e}^{-1.35\tau_0})}{12(\tau_0+2/3)^2} + 0.45{\rm e}^{-3.7\tau_0}\ln\frac{10}{3\tau_0} \tag{16}$$

and for a very low optical depth ($\tau_0 < 0.1$)

$$\beta = \ln\left[\frac{1}{\tau_0\ln(1.53/\tau_0)}\right]. \tag{17}$$

If, on the other hand, we approximate the CENBOL as a spherical bulge, for an optical depth $\tau_0 > 0.1$, β is obtained from

$$\beta = \frac{\pi^2(1-{\rm e}^{-0.7\tau_0})}{3(\tau_0+2/3)^2} + {\rm e}^{-1.4\tau_0}\ln\frac{4}{3\tau_0} \tag{18}$$

and for a very low optical depth ($\tau_0 < 0.1$)

$$\beta = \ln\frac{4}{3\tau_0}. \tag{19}$$

It is important to know the integrated energy of the emitted spectrum (CT95). This is called the Comptonization enhancement factor $\mathcal{F}$. This, as a function of the spectral index α and the effective low-frequency (temperature T_r) dimensionless photon energy $x_0 = 2.7kT_r/kT_{\rm e}$, is given by (CT95)

$$\mathcal{F} = \begin{cases} q_{x_0}(\alpha)x_0^{\alpha-1}, & \text{if } \alpha < 1; \\ \frac{\alpha(\alpha+3)[1-(\alpha+4)/(2\alpha+3)x_0^{\alpha-1}]}{(\alpha+4)(\alpha-1)}, & \text{if } \alpha \geq 1. \end{cases} \tag{20}$$

where

$$q_{x_0}(\alpha) = \frac{\alpha(\alpha+3)\Gamma(\alpha+4)\Gamma(\alpha)\Gamma(1-\alpha)}{\Gamma(2\alpha+4)}(1-x_0^{1-\alpha}).$$

The albedo A_ν of the post-shock region determines the fraction of the intercepted flux scattered away at each radius of the disc. To calculate this factor, we consider the recoil effect and photoelectric absorption. In the presence of the recoil effect only, the incident radiation will be absorbed completely, if (ST80; Titarchuk 1987; CT95)

$$\frac{\Delta\nu}{\nu} \sim \frac{h\nu}{m_{\rm e}c^2}\tau_0^2 = z\tau_0^2 \sim 1, \tag{21}$$

i.e.

$$\tau_0 \sim \frac{1}{z^{1/2}}. \tag{22}$$

The albedo A_ν would be $1 - 1/\tau_0 = 1 - z^{1/2}$. In the presence of absorption, $A_\nu = 1 - 1/\tau_0 = 1 - (\delta_\nu)^{1/2}$, where δ_ν is the probability of the photoelectric absorption (CT95). If we consider both the recoil and the photoelectric absorption, and taking into account the angular dependencies, we get a proper expression (CT95) of albedo:

$$A_\nu = 1 - \phi(\mu_0)\Delta, \tag{23}$$

$$\phi(\mu_0) = \frac{1+\sqrt{3}\mu_0}{1+\sqrt{3}(1-\lambda_\nu)\mu_0} \times \left[1 - \frac{\lambda_\nu\mu_0}{4}(1+\lambda_\nu^2)\Big(\ln\mu_0 + 1.33 - 1.458\mu_0^{0.62}\Big)\right], \tag{24}$$

$$\Delta = (1-\lambda_\nu)^{1/2} = \left[\sqrt{z}\exp(\delta_\nu){\rm erfc}\left(\frac{\delta_\nu^{1/2}}{\sqrt{z}}\right) + \delta_\nu^{1/2}\right], \tag{25}$$

where $\mu = \cos\psi$ and ψ is the angle between the incident radiation and the local normal of the disc. In CT95, the above equations were used for a prescribed flow having a fixed shock location. Presently, we use the above equations in each stage of iteration of the hydrodynamic solution till the complete solution, including the sonic points, and shock locations converge.

2.4 Details of the coupling and solution procedure

In a given run, we assume a Keplerian disc rate ($\dot{m}_{\rm d}$) and a fixed sub-Keplerian halo rate ($\dot{m}_{\rm h}$) with a given set of specific energy (ϵ) and angular momentum (λ). To include cooling in the coupled radiative hydrodynamics code, we follow these steps. (1) As the first step of iteration, we calculate the shock location, inner sonic point and the outer sonic point from the hydro-code following C89 without assuming any radiative transfer. (2) Assuming the emission from the Keplerian disc to be the same as that from a standard Shakura–Sunyaev disc, cooling (heating) of the electrons is computed using the prescription of CT95. This gives us the average electron temperature and the Comptonization enhancement factor. The average electron temperature is obtained after computing

$$g(\tau) = \left(1 - 1.5{\rm e}^{-(\tau_0+2)}\right)\cos\frac{\pi}{2}\left(1 - \frac{\tau}{\tau_0}\right) + 1.5{\rm e}^{-(\tau_0+2)},$$

and using

$$T_{\rm e}(\tau_0) = \frac{\int_0^{\tau_0} T_{\rm e}(\tau)g^2(\tau)(\tau_0-\tau)^2{\rm d}\tau}{\int_0^{\tau_0} g^2(\tau)(\tau_0-\tau)^2{\rm d}\tau}$$

(CT95), where τ_0 is the optical depth of the CENBOL (post-shock region). (3) We calculate the amount of energy loss by the electrons ($\Delta\varepsilon$). (4) We also calculate the albedo A_ν to determine the fraction of the CENBOL flux scattered away at each radius of the disc. The rest $\mathcal{B}_\nu = (1 - A_\nu)$ is assumed to be absorbed by the disc and is re-radiated. Since our model, by definition, includes

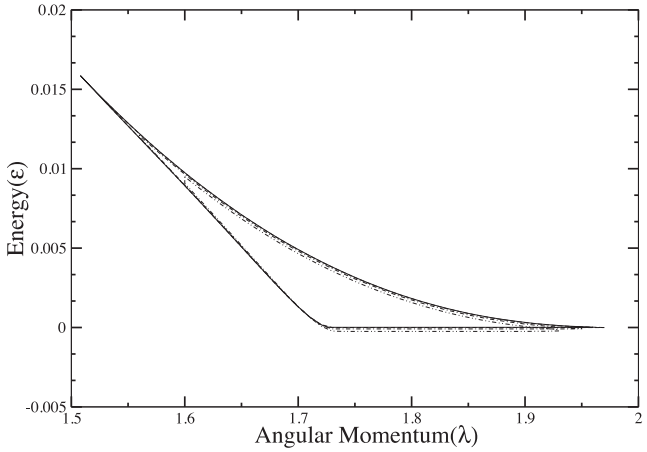

Figure 2. The allowed parameter space in the presence of Comptonization. The solid, dashed and dot–dashed curves are for the non-dissipative flow, for $\dot{m}_{\rm d} = 0.04$ and for $\dot{m}_{\rm d} = 0.15$, respectively. With the increase in the accretion rate, the number of soft photons from the Keplerian disc is increased and thus the amount of cooling increases. This shrinks down the parametric space. Note that flows with negative energy can become transonic in the latter two cases.

the reflected component, we need not add any other reflected component as in often done in other models (e.g. Garcia et al. 2011, and references therein). (5) We then subtract ($\Delta\varepsilon$) from the injected (non-dissipative-flow) energy. We take the new energy as the initial condition and repeat steps (1)–(4) until the spectrum converges iteratively. At the convergence, we get the final shock location, final sonic point locations, as well as the emergent spectrum, spectral index and the full solution of the transonic flow self-consistently. (6) The full procedure is then repeated for every point in the flow parameter space for every pair of disc and halo accretion rates to check which region of the parameter space allows the formation of shocks.

3 RESULTS AND DISCUSSIONS

In C89 and Chakrabarti & Das (2004, hereafter CD04), it was shown that if an ideal flow begins its journey with the conserved specific energy and angular momentum from a certain region of the parameter space, then only the ideal Rankine–Hugoniot conditions are fulfilled and a stable, axisymmetric shock is produced in the flow close to a black hole. We now show the modified parameter space which allows shock formation in the self-consistent transonic flow in the presence of thermal Comptonization. In Fig. 2, we show the variation of the allowed parametric space (spanned by specific energy and angular momentum) for different values of accretion rates. The solid curve is for the non-dissipative flow. The dashed curve is for the accretion rate $\dot{m}_{\rm d} = 0.04$ and the dot–dashed curve is for the accretion rate $\dot{m}_{\rm d} = 0.15$ of the Eddington rate. The sub-Keplerian halo rate is $\dot{m}_{\rm h} = 1$. This shows that the parametric space decreases self-consistently with increasing accretion rate. The parametric space decreases significantly from the low angular momentum side because of the drop of pressure due to cooling effects. In other words, the shocks can form only if the angular momentum is significant and close to the marginally stable value. Most interestingly, we note that transonic solutions are possible even for negative flow energy, i.e. for bound flows.

Figs 3(a) and (b) show that if we increase the accretion rate ($\dot{m}_{\rm d}$) (a) the cooling increases and (b) the shock moves towards the black hole when the initial flow has an identical set of specific energy and specific angular momentum ($\varepsilon = 0.0021, \lambda = 1.74$). Here, the shock is in the unit of $r_{\rm s}$. We chose the halo rate $\dot{m}_{\rm h} = 1$ and the mass of the black hole $M = 5\,{\rm M}_{\odot}$. As the Keplerian disc accretion rate rises, the thermal Comptonization is more effective and the cooling of the electrons is more efficient. As a result, the pressure in the post-shock region drops. To satisfy the modified Rankine–Hugoniot condition, the shock moves towards the black hole.

In Fig. 4(a), we show the variation of the energy spectrum with increase of the Keplerian disc accretion rate, keeping the halo rate $\dot{m}_{\rm h} = 1$, initial energy $\varepsilon = 0.0021$ and angular momentum of the flow $\lambda = 1.74$ fixed. The solid, dotted and dot–dashed curves show the spectra for $\dot{m}_{\rm d} = 0.001$ (A), 0.04 (B) and 0.15 (C), respectively. Clearly, the spectrum becomes softer for higher values of $\dot{m}_{\rm d}$ as it increases the number of injected soft photons which cool down the CENBOL faster. For a comparison, we show the CT95 solution of these cases where the transonic solution did not include Comptonization in computing the shock location. While the general trend remains the same, the difference is due to the variation in shock temperature and shock height. We observe that apart from being of low intensity, the spectrum is softer. As the CENBOL size is smaller, it is easier to cool. This is reflected in the computation

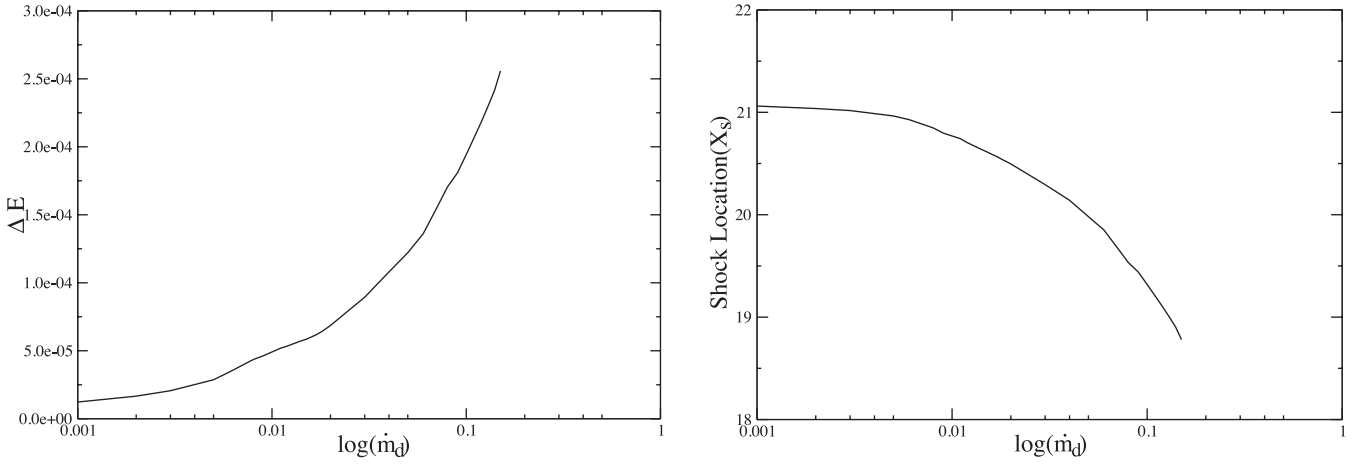

Figure 3. Variation of (a) the lost energy $\Delta\varepsilon$ due to cooling from the post-shock region due to Comptonization and (b) the shock location as a function of the disc accretion rate ($\dot{m}_{\rm d}$). Clearly, $\Delta\varepsilon$ increases with $\dot{m}_{\rm d}$.

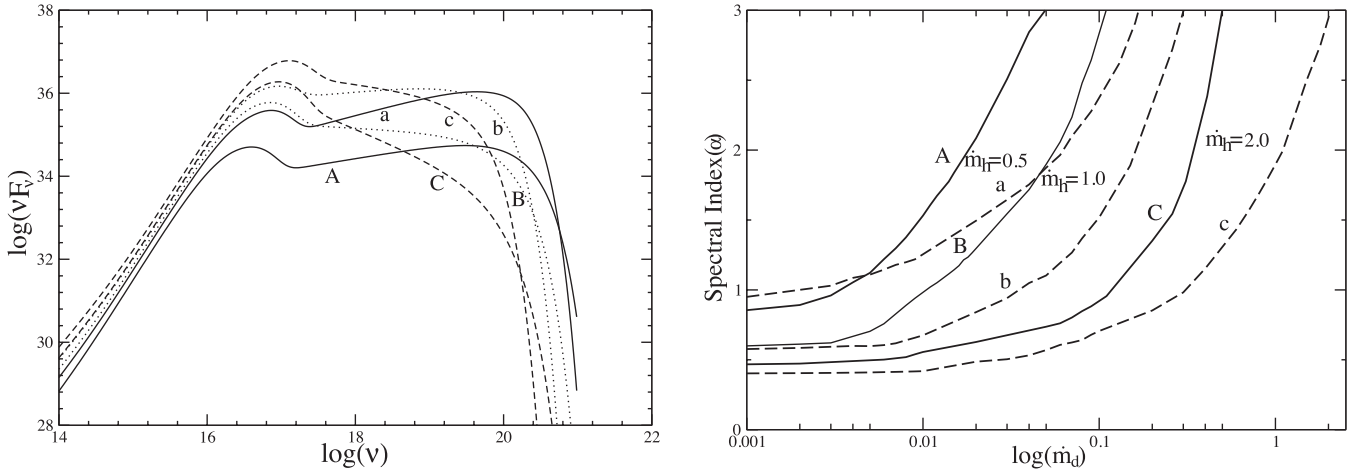

Figure 4. (a) Variation of the spectrum with the increase of the accretion rate, keeping the halo rate ($\dot{m}_{\rm h} = 1$), initial (non-dissipative) energy ($\varepsilon = 0.0021$) and angular momentum of the flow ($\lambda = 1.74$) fixed. The solid, dotted and dashed curves show the softening of the spectra for $\dot{m}_{\rm d} = 0.001$, 0.04 and 0.15, respectively. (b) Variation of spectral index (α) with the accretion rate ($\dot{m}_{\rm d}$) for different halo rates.

of the spectral index also. In Fig. 4(b), we show the variation of spectral index (α) with accretion rates ($\dot{m}_{\rm d}$ and $\dot{m}_{\rm h}$). The curves are in general shifted upwards, since the spectra are softer. For example, when $\dot{m}_{\rm h} = 1.0$, the hard-to-soft transition ($\alpha = 1$) takes place at $\dot{m}_{\rm d} = 0.011$ instead of at 0.033 valid for a non-dissipative transonic flow. If we decrease the halo rate, the optical depth of the post-shock region is decreased, thereby decreasing the number of hot electrons in the post-shock region to process the intercepted soft photons which makes the spectrum softer. Note that when the disc rate is very low, the spectral index is very insensitive to the disc rate. However, since thermal Comptonization becomes effective when the CENBOL optical depth is above $\sim 2/3$, the cooling takes effect suddenly and the soft state is formed. With the rise in the disc rate, the cooling rate becomes higher and thus the change in the parameter space forming shocks is also rapid (Fig. 2).

In Fig. 5, we show the variation of the mean electron temperature (in keV) in the presence of thermal Comptonization as a function of disc accretion rate (x-axis) for an initial set of energy (0.0021) and angular momentum (1.74) when the halo rate ($\dot{m}_{\rm h}$) is varied. With

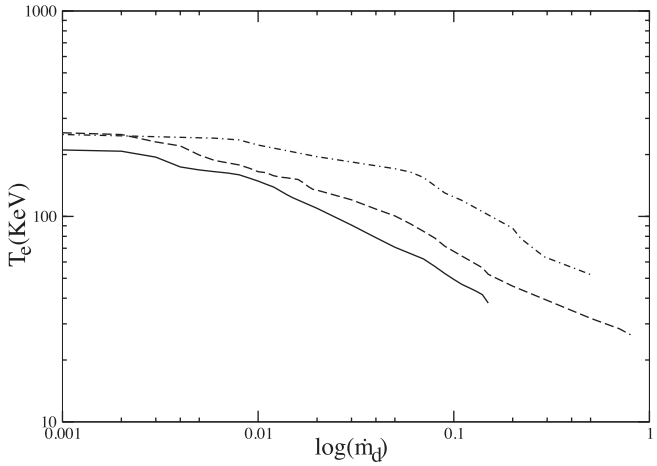

Figure 5. Variation of the mean electron temperature (in keV) of the CENBOL in the presence of Comptonization as a function of the disc accretion rate (x-axis) for a set of energy and angular momentum when the halo rate ($\dot{m}_{\rm h}$) is different.

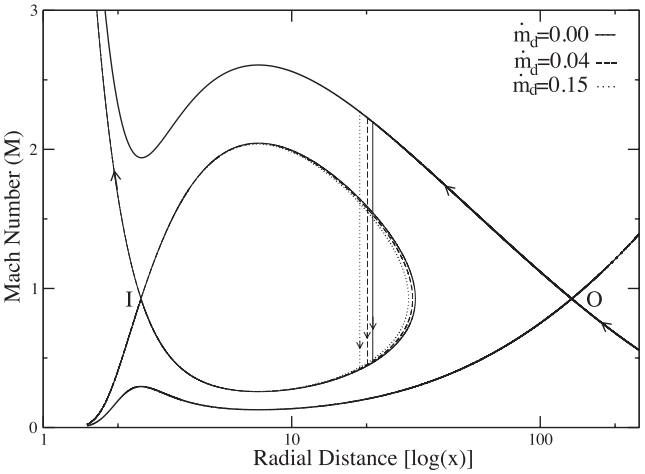

Figure 6. Example of a complete solution of the accretion flow in the M–$\log(x)$ plane. As the accretion rate increases, the shock moves closer to the black hole. See the text for details.

the increase of the disc accretion rate, the mean electron temperature decreases when the halo rate is fixed: $\dot{m}_{\rm h}$ = is 0.5 (solid curve), 1.0 (dashed curve) and 2.0 (dot–dashed curve). As in the case of spectral index, the temperature remains insensitive to the disc accretion rate as long that the CENBOL optical depth is not high enough. For higher accretion rates, the CENBOL cools rather rapidly as in CT95.

In Fig. 6, we show an example of a complete solution in the presence of Comptonization inside the CENBOL. We present the variation of Mach number with logarithmic radial distance. We note that the shock moves towards the black hole as the cooling rises due to cooling effects in the post-shock region (see also CD04; Das & Chakrabarti 2004; Das et al. 2010). The solid curve is for the non-dissipative flow where the specific energy is 0.0021 and the specific angular momentum is 1.74. The dashed and dotted curves are for the accretion rates $\dot{m}_{\rm d} = 0.04$ and 0.15, respectively. The halo rate is 1.0. The vertical lines show the shock transitions at $x_{\rm s}$ ($x_{\rm s3}$ in C89): $x_{\rm s} = 21.188$ (solid curve), $x_{\rm s} = 20.182$ (dashed curve) and $x_{\rm s} = 18.780$ (dotted curve).

4 SUMMARY AND DISCUSSIONS

In this paper, for the first time, we introduce thermal Comptonization in the study of the properties of a transonic flow around a black hole. We also study the formation of standing shocks. For Comptonization, we need to have the source of seed photons. For this, we assume a TCAF of CT95 where a viscous, standard Keplerian disc in the equatorial plane supplies the seed photons in the form of soft X-rays. The hot electrons in the post-shock region (CENBOL acting as the Compton cloud) of a low angular momentum and low viscosity flow (halo) which surrounds the Keplerian disc interact with these seed photons and energize them through inverse Comptonization to produce hard X-rays. In this condition, as the accretion rate of the Keplerian disc is increased, the soft photon flux is increased, and the Compton cloud is cooled, resulting in softening the spectrum. As the halo rate is increased, the hot electron density goes up, hardening the spectrum. We study the parameter space in which standing shocks in a Comptonized transonic flow form. We find that Comptonization reduces the parameter space for positive initial energy of the flow, but increases it for negative energy (i.e. in bound orbits). We use our self-consistent solution for a TCAF and obtain the emerging spectrum. The cooling of the post-shock region reduces the post-shock pressure and pushes the shock towards the black hole. This reduces the CENBOL size and thus the cooling in our self-consistent flow is higher than what was envisaged in the CT95 model. The major difference between our present paper and CT95 is that in CT95, the shock and the proton temperature in the pre-shock flow were prescribed before the spectrum was obtained. Presently, the entire solution, including the shock location, comes out self-consistently.

The post-shock region, or the CENBOL, not only produces observed hard X-rays (CT95), but also supplies matter for the jet and the outflow (Chakrabarti 1999). The inverse Compton process mainly removes the thermal energy of the inflow. As the radiative loss decreases thermal pressure, it not only reduces the CENBOL size, but also reduces the outflow rate. In Das et al. (2010), where an unspecified type of energy loss was assumed to be instantaneously taking place at the shock, a similar behaviour of the parameter space was observed and the shock location behaved qualitatively in the same way. Our present paper considers distributed loss of energy all over the CENBOL and therefore our study is complementary in nature.

In this paper, we concentrated on obtaining the effects of cooling by inverse thermal Comptonization. It is well known that the innermost region of the disc is rapidly falling in and is in fact supersonic (C89; CT95). At high accretion rates, when the flow becomes cold and the thermal Comptonization can be ignored, the bulk motion causes the energy shift of seed photons. This so-called bulk-motion Comptonization spectrum is decided by the upper limit of the velocity of matter, namely the velocity of light, and thus the spectral slope saturates to around 2.0 even when the rates are varied. The theoretical works (CT95; Titarchuk & Zannias 1998), Monte Carlo simulations (Laurent & Titarchuk 1999) and the observational results (Shaposhnikov & Titarchuk 2009, Titarchuk & Seifina 2009) all point to these saturation effects. Since this property is solely due to the unique properties of a black hole accretion, this is not affected by our analysis of thermal Comptonization, valid for lower accretion rates of the Keplerian component.

ACKNOWLEDGEMENT

SM acknowledges a CSIR Fellowship for this work.

REFERENCES

Chakrabarti S. K., 1989, ApJ, 347, 365 (C89)
Chakrabarti S. K., 1990a, ApJ, 350, 275 (C90a)
Chakrabarti S. K., 1990b, Theory of Transonic Astrophysical Flows. World Scientific, Singapore (C90b)
Chakrabarti S. K., 1990c, MNRAS, 243, 61 (C90c)
Chakrabarti S. K., 1996a, Phys. Rep., 266, 229
Chakrabarti S. K., 1996b, ApJ, 464, 664
Chakrabarti S. K., 1998, preprint (astro-ph/9812140)
Chakrabarti S. K., 1999, A&A, 351, 185
Chakrabarti S. K., Das S., 2004, MNRAS, 349, 649 (CD04)
Chakrabarti S. K., Titarchuk L. G., 1995, ApJ, 455, 623 (CT95)
Das S., Chakrabarti S. K., 2004, Int. J. Mod. Phys. D, 13, 1955
Das S., Chakrabarti S. K., Mondal S., 2010, MNRAS, 401, 2053
Garcia J., Kallman T. R., Mushotzky R. F., 2011, ApJ, 731, 131
Giri K., Chakrabarti S. K., 2013, MNRAS, in press
Haardt F., Maraschi L., 1993, ApJ, 413, 507
Kobayashi Y., Kubota A., Nakazawa K., Takahashi T., Makishima K., 2003, PASJ, 55, 273
Lang K. R., 1980, Astrophysical Formula. Springer, New York
Laurent P., Titarchuk L., 1999, ApJ, 511, 289
Laurent P., Titarchuk L. G., 2011, ApJ, 727, 34
Liang E. P., Thompson K. A., 1980, ApJ, 240, 271
Matsumoto R., Kato S., Fukue J., Okazaki A. T., 1984, PASJ, 36, 71
Molteni D., Sponholz H., Chakrabarti S. K., 1996, ApJ, 457, 805
Novikov I., Thorne K. S., 1973, in DeWitt C., DeWitt B. S., eds, Black Holes. Gordon & Breach, New York, p. 343
Paczyński B., Bisnovatyi-Kogan G., 1981, Acta Astron., 31, 283
Paczyński B., Witta P. J., 1980, A&A, 88, 23
Shakura N. I., Sunyaev R. A., 1973, A&A, 24, 337 (SS73)
Shapiro S., Teukolosky S., 1984, Black Holes, Neutron Stars and White Dwarfs. John Wiley & Sons, New York
Shaposhnikov N., Titarchuk L. G., 2009, ApJ, 699, 453
Singh C. B., Chakrabarti S. K., 2011, MNRAS, 410, 2414
Sunyaev R. A., Titarchuk L. G., 1980, ApJ, 86, 121 (ST80)
Sunyaev R. A., Titarchuk L. G., 1985, A&A, 143, 374 (ST85)
Titarchuk L. G., 1987, Sov. Astrofiz., 26, 57
Titarchuk L. G., 1994, ApJ, 434, 570
Titarchuk L. G., Lyubarskij Y., 1995, ApJ, 450, 876
Titarchuk L. G., Seifina E., 2009, ApJ, 706, 1463
Titarchuk L. G., Zannias T., 1998, ApJ, 493, 863
Zdziarski A. A., Lubinski P., Gilfanov M., Revnitsev M., 2003, MNRAS, 342, 355

This paper has been typeset from a TEX/LATEX file prepared by the author.